

phys. stat. sol. (a) **176**, 401 (1999)

Subject classification: 68.55.Jk; 68.55.Ln; S7.14

Influence of Si Doping on the Subgrain Structure of GaN Grown on AlN/Si(111)

S. I. MOLINA¹) (a), A. M. SÁNCHEZ (a), F. J. PACHECO (a), R. GARCÍA (a),
M. A. SÁNCHEZ-GARCÍA (b), and E. CALLEJA (b)

(a) *Departamento de Ciencia de los Materiales e Ingeniería Metalúrgica y Química Inorgánica, Universidad de Cádiz, Apdo. 40, E-11510 Puerto Real (Cádiz), Spain*

(b) *Departamento de Ingeniería Electrónica, ETSI Telecomunicación, UPM, Ciudad Universitaria s/n, E-28040 Madrid, Spain*

(Received July 4, 1999)

This work presents a detailed study of the subgrain structure of Si doped GaN grown on AlN buffered (111)Si substrates by plasma-assisted Molecular Beam Epitaxy. Si doping increases from an unintentionally undoped sample up to $1.7 \times 10^{19} \text{ cm}^{-3}$. The subgrain size distribution fits quite precisely a Gaussian distribution for the undoped sample. The asymmetry and standard deviation of such distribution increases with Si doping. The average subgrain size decreases as the Si doping increases. Its value is 177 nm for a Si doping of $6.0 \times 10^{18} \text{ cm}^{-3}$ and it increases up to 282 nm for the undoped sample. On the other hand, though the subgrain boundaries appear to be free of any precipitate in the nominally undoped sample, particles of a few nm^2 have been observed at the boundaries between the subgrains of the Si doped films.

1. Introduction

Structural, optical and electrical properties of Si doped GaN have been proven to depend on the Si doping level [1 to 5]. The understanding of these properties is fundamental for designing optoelectronic and electronic devices based on GaN. In particular, Si doping of GaN grown on AlN buffered (111)Si substrates by plasma-assisted Molecular Beam Epitaxy promotes an enhancement of the biaxial strain in the film [6] and a strong reduction of the dislocation density reaching the free surface [7, 8]. These effects are associated with significant changes in the structure of subgrains that constitute the mosaic structure of the GaN film.

In this work, the influence of the Si doping on size, shape, misorientation and boundaries of the subgrains in GaN:Si grown by plasma-assisted molecular beam epitaxy (MBE) on AlN buffered (111)Si substrates is studied by plan view and cross section transmission electron microscopy (TEM), selected area electron diffraction (SAED) and high resolution electron microscopy (HREM).

2. Experimental

Si doped GaN layers were grown by plasma-assisted Molecular Beam Epitaxy (MBE) on AlN buffered p-type Si(111) on axis substrates. Si doping ranges between

¹) Corresponding author; Tel.: 34-956-83-08-28; Fax: 34-956-83-49-24;
e-mail: sergio.molina@uca.es

$n_{\text{Si}} = 1.1 \times 10^{17} \text{ cm}^{-3}$ and $n_{\text{Si}} = 1.7 \times 10^{19} \text{ cm}^{-3}$. As a reference sample, an undoped sample has been grown under similar growth conditions. The GaN growth temperature was 760°C and the thickness of this layer is $0.8 \mu\text{m}$. Further details on the growth system and conditions were published elsewhere [9 to 11]. Preparation of TEM specimens was performed by mechanical thinning and ion milling using optimised conditions for GaN. Samples were studied by TEM, HREM and associated techniques using cross sectional (XTEM) and plan view (PVTEM) orientations with the transmission electron microscopes Jeol 1200 EX and 2000 EX.

3. Results and Discussion

The defect structure of the Si doped GaN layers presented in this work was studied elsewhere [7, 8]. The GaN layer consists of a mosaic structure where subgrains are slightly misoriented. This layer has the hexagonal wurtzite crystalline structure oriented with its [1120] parallel to the Si[110] and its [0001] parallel to the Si[111]. The density of dislocations that reach the free surface of the GaN layer decreases with the Si doping, while the planar defect density and the out-plane misorientation angle between the subgrains of this layer follow an opposite trend [8]. The present work concentrates in the subgrain structure that constitute the mosaic structure of the GaN layer.

In order to quantify the subgrain size distribution, several series of PVTEM images have been recorded for each studied sample by tilting the specimens. This analysis has been done with the AMTTM-VIDS V semiautomatic image analysis system of Synoptics. The analyzed regions include hundreds of subgrains. Fig. 1 shows the obtained subgrain size distribution for an undoped GaN/AlN/Si(111) (Fig. 1a) and two Si doped samples (Fig. 1b, $n_{\text{Si}} = 1.1 \times 10^{17} \text{ cm}^{-3}$, and Fig. 1c, $n_{\text{Si}} = 6.0 \times 10^{18} \text{ cm}^{-3}$). The subgrain size distribution fits quite precisely a gaussian distribution for the undoped sample. The

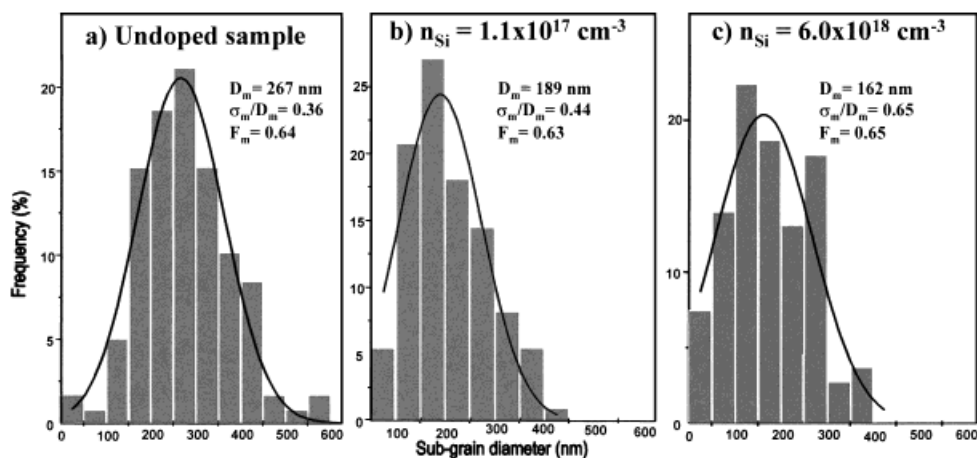


Fig. 1. Subgrain size distribution for a) the undoped and Si doped samples: b) $n_{\text{Si}} = 1.1 \times 10^{17} \text{ cm}^{-3}$ and c) $n_{\text{Si}} = 6.0 \times 10^{18} \text{ cm}^{-3}$. For each sample the values of the average subgrain size (D_m), the relationship between the standard deviation of the size distribution and D_m (σ_m/D_m) and the average subgrain shape factor (F_m) are indicated. The subgrain sizes are expressed as the subgrain diameter assuming a circle with an area equal to the measured area of subgrains. The shape factor is equal to one if the subgrain shape is a circle

asymmetry and the relative standard deviation (σ_m/D_m) of this distribution increases with Si doping. On the contrary, the average subgrain size decreases as the Si doping increases. However, the shape factor of the subgrain distribution is similar both for Si doped and undoped samples.

The subgrains that configure the mosaic structure of GaN are slightly misoriented both in- and out- (0001) growth plane. By analyzing electron microdiffraction patterns recorded from adjacent subgrains in plan view and cross section prepared specimens, the out-plane misorientation resulted to increase with the Si doping [7]. On the other hand, the in-plane misorientation has been estimated from plan view SAED patterns recorded from areas of $66 \mu\text{m}^2$. As observed in the SAED pattern of the undoped sample (see Fig. 2a), the diffracted spots have curved and elongated shapes instead of

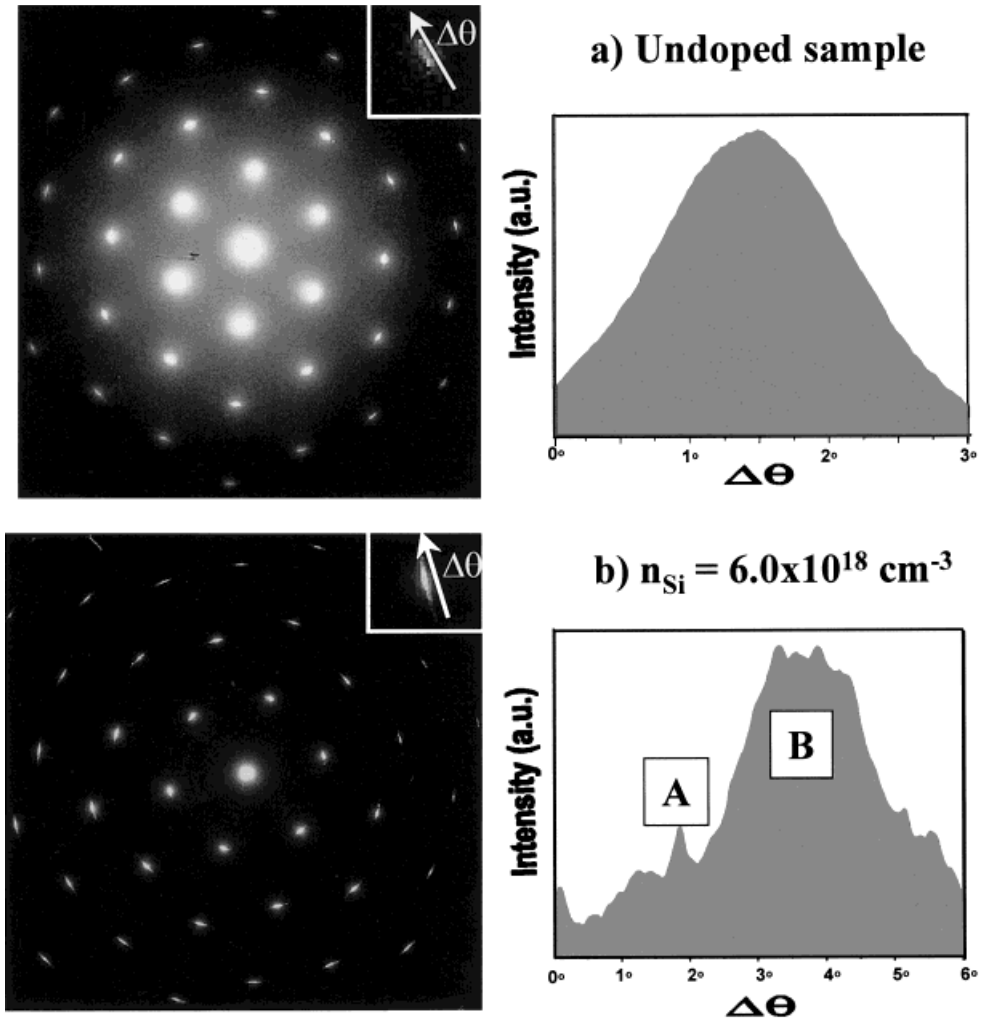


Fig. 2. Profiles of intensity along a selected elongated shape spot of the plan view SAED pattern recorded in a) the undoped and b) Si doped sample with $n_{\text{Si}} = 6.0 \times 10^{18} \text{ cm}^{-3}$

circular shapes. The measurement of the arc that such curved spots occupy is related with the in-plane misorientation of the subgrains. For Si doping up to $1.1 \times 10^{17} \text{ cm}^{-3}$, the intensity profile through the curved-shape elongated spots is quite symmetrical fitting a single Gaussian function, as shown in Fig. 2a. Similar measurements in samples with Si doping larger than $n_{\text{Si}} = 5.0 \times 10^{18} \text{ cm}^{-3}$ show a quite disperse distribution of in-plane subgrain misorientations, as shown in the intensity profile of Fig. 2b, unlike of that observed in undoped and low Si doping level ($n_{\text{Si}} = 1.1 \times 10^{17} \text{ cm}^{-3}$). The peaks, such as that one marked with the letter A in the profile of Fig. 2b, correspond to subgrains which possess infrequent misorientations in the region of the plan view examined sample. However, the majority of the misorientations of the subgrains in sample with $n_{\text{Si}} = 6.0 \times 10^{18} \text{ cm}^{-3}$ are grouped around a maximum value (see peak B in Fig. 2b), though its distribution is again quite asymmetrical and the fit accuracy to a Gaussian function is poor compared to the above mentioned samples (undoped and doped sample with $n_{\text{Si}} = 1.1 \times 10^{17} \text{ cm}^{-3}$). These findings show that Si doping increases the inhomogeneity of the subgrain misorientation distribution.

Finally, some subgrains have been found to be rotated 30° around [0001] with respect to the hexagonal GaN matrix as determined by PVTEM, HREM and SAED. Such rotated subgrains were exceptionally observed in the undoped sample and they are found more frequently as the doping rate increases. Fig. 3 shows a HREM image of one of these rotated subgrains and its boundary with another GaN subgrain.

Some crystalline particles have been found to be located in the subgrain boundaries of the Si doped samples. The HREM image of Fig. 4 has been recorded from one of these particles included in a grain boundary. The interfacial particle is disoriented $1.0^\circ \pm 0.5^\circ$ with respect to the adjacent grains. The analysis of this HREM image reveals that the boundary between the interfacial crystallite and the adjacent grains is not coherent along its whole length. To accommodate a tilt boundary of $1.0^\circ \pm 0.5^\circ$ in hexagonal GaN the presence of one dislocation with $\mathbf{b} = \mathbf{a}_{\text{hexagonal GaN}}$ is necessary at the

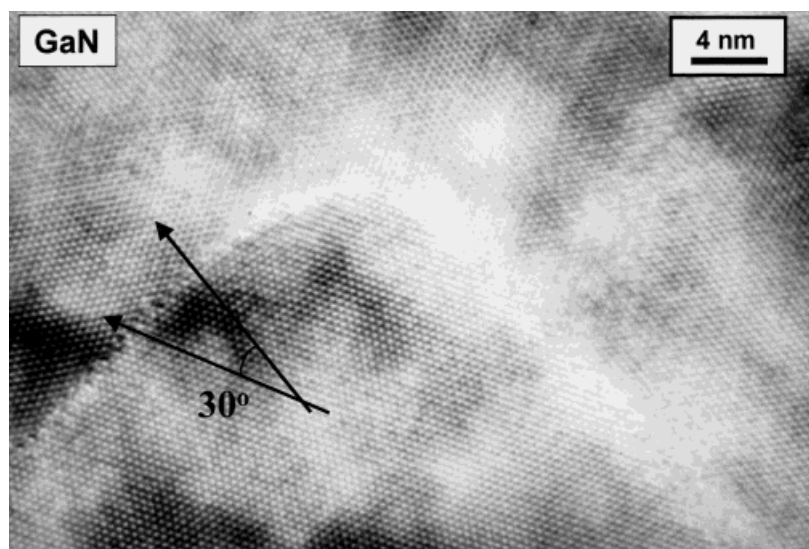


Fig. 3. HREM image of a subgrain rotated 30° around GaN[0001]

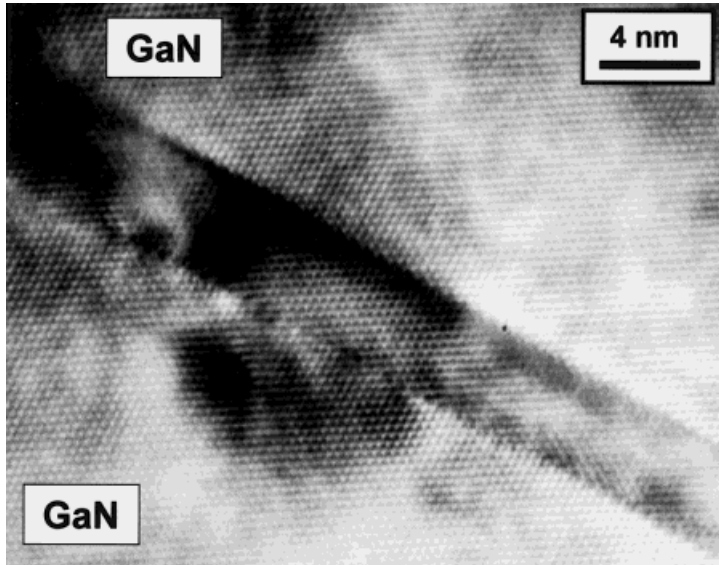


Fig. 4. HREM image of a particle located at a subgrain boundary

boundary each (24.2 ± 12.2) nm. This observation is explained assuming that the particle consists of hexagonal GaN and that dislocations are associated to a tilt boundary between the grains and the particle. However, the possibility that such interfacial particles consist of a cubic phase along [111] cannot be completely discarded.

4. Conclusions

The distribution of subgrains constituting the mosaic structure of GaN grown on AlN buffered (111)Si substrates by plasma-assisted Molecular Beam Epitaxy is strongly modified by Si doping of the grown film. Si doping originates an increase of the asymmetry and the relative standard deviation of such distribution, and a decrease both of the subgrain size and the homogeneity degree of the subgrain misorientation distribution. On the other hand, particles of a few nm² exist in the boundaries between the Si doped GaN subgrains.

Acknowledgements This work has been supported by CICYT Project MAT98-0823-C03-02 and Junta de Andalucía (Group PAI TEP 0120). The group from Madrid wishes to acknowledge the financial support provided by Project No. EU ESPRIT LTR 20968 (Laquani).

References

- [1] E. OH, H. PARK, and Y. PARK, *Appl. Phys. Lett.* **72**, 1848 (1998).
- [2] E. F. SCHUBERT, I. D. GOEFFERT, W. GRIESHABER, and J. M. REDWING, *Appl. Phys. Lett.* **71**, 921 (1997).
- [3] IN-HWAN LEE, IN-HOON CHOI, C. R. LEE, and S. K. NOH, *Appl. Phys. Lett.* **71**, 1359 (1997).
- [4] S. RUVIMOV, Z. LILIENTAL-WEBER, T. SUSKI, J. W. AGER III, J. WASHBURN, J. KRUEGER, C. KISIELOWSKI, E. R. WEBER, H. AMANO, and I. AKASAKI, *Appl. Phys. Lett.* **69**, 990 (1996).

- [5] X. ZHANG, SOO-JIN CHUA, W. LIU, and KOK-BOON CHONG, *Appl. Phys. Lett.* **72**, 1890 (1998).
- [6] E. CALLEJA, M. A. SÁNCHEZ-GARCÍA, F. J. SÁNCHEZ, F. CALLE, F. B. NARANJO, E. MUÑOZ, S. I. MOLINA, A. M. SÁNCHEZ, F. J. PACHECO, and R. GARCÍA, *J. Cryst. Growth* **202**, 296 (1999).
- [7] S. I. MOLINA, A. M. SÁNCHEZ, F. J. PACHECO, R. GARCÍA, M. A. SÁNCHEZ-GARCÍA, and E. CALLEJA, in: *Lattice-Mismatched Thin Film*, Ed. E. A. FITZGERALD, Warrendale (PA), accepted for publication.
- [8] S. I. MOLINA, A. M. SÁNCHEZ, F. J. PACHECO, R. GARCÍA, M. A. SÁNCHEZ-GARCÍA, F. J. SÁNCHEZ, and E. CALLEJA, *Appl. Phys. Lett.* **74**, 3362 (1999).
- [9] M. A. SÁNCHEZ-GARCÍA, E. CALLEJA, F. J. SÁNCHEZ, F. CALLE, E. MONROY, D. BASAK, E. MUÑOZ, C. VILLAR, A. SANZ-HERVAS, M. AGUILAR, J. J. SERRANO, and J. M. BLANCO, *J. Electron. Mater.* **27**, 276 (1998).
- [10] E. CALLEJA, M. A. SÁNCHEZ-GARCÍA, E. MONROY, F. J. SÁNCHEZ, E. MUÑOZ, A. SANZ-HERVAS, C. VILLAR, and M. AGUILAR, *J. Appl. Phys.* **82**, 4681 (1997).
- [11] M. A. SÁNCHEZ-GARCÍA, E. CALLEJA, E. MONROY, F. J. SÁNCHEZ, F. CALLE, E. MUÑOZ, and R. BERSFORD, *J. Cryst. Growth* **183**, 23 (1998).